ACKNOWLEDGMENT

The authors wish to thank Dr. C. Pottle of the Cornell University School of Electrical Engineering for help in the preparation of the English text of this paper. The calculations were carried out at the computing center of the Technical University of Aachen, Germany.

REFERENCES

[1] W. E. Thomson, "Networks with maximally flat delay," *Wireless Engrg.*, vol. 29, pp. 256–263; October 1952.
[2] ——, "The synthesis of a network to have a sine-squared impulse response," *Proc. IEE (London)*, pt. III, vol. 29, pp. 373–376; 1952.
[3] F. A. Muller, "High-frequency compensation of *RC* amplifiers," *Proc. IRE*, vol. 42, pp. 1271–1276; August 1954.
[4] H. H. Voss, "Realisierbare Tiefpässe und Bandpässe minimaler Phase mit geebneter Laufzeit und aperiodischem Einschwing verhalten," *Frequenz*, vol. 8, pp. 97–102; April 1954.
[5] J. A. Villes and J. Bouzitat, "Sur un type de signaux practiquement bornés en temp et en frequence," *Cables et Transmissions*, vol. 9, pp. 293–303; October 1955.
[6] Y. Peless and T. Murakami, "Analysis and synthesis of transitional Butterworth-Thomson filters and bandpass amplifiers," *RCA Rev.*, vol. 18, pp. 60–94; March 1957.
[7] W. Poschenrieder and H. Sontheim, "Ein Analogiegerät für Aufgaben der Filterentwicklung," *Frequenz*, vol. 13, pp. 379–385; December 1959.
[8] S. K. Mullick, "Pulse networks with parabolic distributions of poles," *IRE Trans. on Circuit Theory*, vol. CT-9, pp. 302–305; September 1961.
[9] K. Uhl, "Ein Filtersystem mit günstigen Impulseigenschaften," *Archiv der elektrischen Übertragung (AEÜ)*, vol. 15, pp. 109–114; March 1961.
[10] O. Herrmann and H. W. Schüssler, "Zur Auswahl von Filtern mit günstigem Einschwingverhalten," *AEÜ*, vol. 14, pp. 183–189; April 1960.
[11] J. Jess and H. W. Schüssler, "Über Filter mit günstigem Einschwingverhalten," *AEÜ*, vol. 16, pp. 117–128; March 1962.
[12] O. Herrmann, J. Jess, and H. W. Schüssler, "Zur Auswahl optimaler impulsformender Netzwerke," Forschungsbericht Nr. 1081 des Landes Nordrhein-Westfalen, Westdeutscher Verlag Köln und Opladen; 1962.
[13] J. Jess, "Über die Synthese von Impulsformern mit vorgeschriebenen Schranken im Zeit- und Frequenzbereich," Ph.D. dissertation, Technische Hochschule, Aachen, Germany, 1962.
[14] J. Jess, "Über Impulsfilter mit Tschebyscheffschem Verhalten im Zeit- und Frequenzbereich," *AEÜ*, vol. 17, pp. 391–401; August 1963.
[15] A. Papoulis, *The Fourier Integral and its Applications.* New York: McGraw-Hill, 1962, Ch. 4-4.
[16] K. Küpfmüller, *Die Systemtheorie der elektrischen Nachrichtenübertragung.* S. Hirzel-Verlag: Stuttgart, 1952, p. 62.
[17] W. Postl, Ein Energiekriterium zur Beurteilung von Impulsfiltern, *AEÜ*, vol. 16, pp. 351–355; July 1962.
[18] J. R. Klauder, A. C. Price, S. Darlington, and W. J. Albersheim "The theory and design of chirp radars," *Bell Sys. Tech. J.*, vol. 39, pp. 745–808; July 1960.
[19] C. L. Dolph, "A current distribution for broadside arrays which optimizes the relationship between beam width and side-lobe level," *Proc. IRE*, vol. 34, pp. 335–348; June 1946.
[20] T. T. Taylor, "Design of line-source antennas for narrow beamwidth and low side lobes," *IRE Trans. on Antennas and Propagation*, vol. AP-3, pp. 16–28; January 1955.
[21] H. W. Schüssler, "Schaltung und Messung von Übertragungsfunktionen am Analogrechner," *AEÜ*, vol. 13, pp. 405–419; October 1959.
[22] F. A. Willers, "Methoden der praktischen Analysis," Göschens Lehrbücherei Band 12, Berlin, Germany, 1950.
[23] J. Jess, "Katalog normierter Tiefpassübertragungsfunktionen mit Tschebyscheffverhalten der Impulsantwort und der Dämpfung," Forschungsbericht Nr. 1329 des Landes Nordrhein-Westfalen, Westdeutscher Verlag Köln und Opladen; 1964.
[24] J. Jess and H. W. Schüssler, "A Class of pulse-forming networks," *IEEE Trans. on Circuit Theory (Correspondence)*, vol. CT-12, pp. 296–299, June 1965.

Bistable Transmission Lines

J. NAGUMO, MEMBER, IEEE, S. YOSHIZAWA, MEMBER, IEEE, AND S. ARIMOTO, MEMBER, IEEE

***Abstract*—The paper introduces two types of active transmission lines having two stable states of equilibrium. In these, a transition from one state to the other is transmitted along the line and the transition waveforms are shaped during transmission. The properties of the lines have been investigated theoretically, using computers, and experimentally by using lumped constant elements and tunnel diodes.**

I. INTRODUCTION

It is KNOWN that some active transmission lines have the property of shaping signal waveforms during their transmission. In other words, each of these transmission lines has a specific waveform peculiar to that line, and a signal waveform, transmitted along the line, approaches the specific waveform asymptotically.

Manuscript received August 5, 1964; revised February 8, 1965.
The authors are with the Dept. of Mathematical Engineering and Instrumentation Physics, University of Tokyo, Tokyo, Japan.

As an example of these active transmission lines, Nagumo, et al. have described an active pulse transmission line with one stable equilibrium state (monostable line) simulating a nerve axon [1]. In this paper we shall discuss active transmission lines with two stable equilibrium states (bistable lines). In these lines, a transition from one state to the other is transmitted along the line; we regard this as a traveling signal.

We shall propose two types of bistable lines, beginning with the simpler one, and discuss their relationship.

II. BISTABLE LINE (*A*)

A. The Circuit and its Equation

We shall consider the circuit in Fig. 1, where TD is a tunnel diode with the characteristic curve shown in Fig. 2. Set the bias voltage E and the resistance R so that this circuit acts as a bistable circuit. In this case, the middle intersection in Fig. 2 is an unstable equilibrium point whereas the other two intersections are both stable.

The equation of this circuit is given by

$$\begin{cases} j = C \dfrac{dv}{d\tau} + g(v), \\ g(v) = f(v) + \dfrac{v - E}{R}, \end{cases} \tag{1}$$

where $I = f(v)$ represents the characteristic curve of the tunnel diode (Fig. 2). Hence, in general, the function $g(v)$ takes the form shown in Fig. 3.

Let $g(v)$ be represented by a third-order polynomial:

$$g(v) = a(v - v_1)(v - v_2)(v - v_3), \tag{2}$$

where $a > 0$ and $v_1 < v_2 < v_3$.

Consider the circuit shown in Fig. 4, which is constructed by cascading many of the two-terminal circuits in Fig. 1 through interstage coupling resistances.

Regarding the foregoing circuit as a distributed line, we find that

$$j = \frac{1}{r} \frac{\partial^2 v}{\partial s^2}, \tag{3}$$

where s is the distance along the line and r the interstage coupling resistance per unit length of the line.

Introducing new variables:

$$t = \frac{a(v_3 - v_1)^2}{4C} \tau, \quad x = \frac{\sqrt{ar}}{2} (v_3 - v_1)s,$$

$$u = 2 \frac{v - v_1}{v_3 - v_1} - 1, \; m = \frac{2v_2 - (v_1 + v_3)}{v_3 - v_1} \; (1 > m > -1), \tag{4}$$

we have, from (1), (2), (3), and (4), the following fundamental equation:

$$\boxed{\frac{\partial^2 u}{\partial x^2} = \frac{\partial u}{\partial t} + (u + 1)(u - m)(u - 1).} \tag{5}$$

Notice that one may assume without loss of generality that

$$0 \geqq m > -1,$$

since if $1 > m > 0$ in (5), replacing u by $-u$, it reduces to the case where $0 \geqq m > -1$.

B. Propagation of Transition

Equation (5) has three constant solutions: $u = -1$, 1, and m. Of these, the first two correspond to the stable equilibrium states, the latter to the unstable equilibrium state.

Initially keeping the line in the stable equilibrium state $u = -1$, an appropriate input applied at one end of the line will cause a transition of the state at that end from $u = -1$ to the other stable equilibrium state $u = 1$. Does the transition of the state from $u = -1$ to $u = 1$ travel along the line?

An answer to this question is given by solving the following boundary-value problem (Fig. 5).

$$\begin{cases} u = u(x, t), \qquad x \geqq 0, \qquad t \geqq 0; \\ \dfrac{\partial^2 u}{\partial x^2} = \dfrac{\partial u}{\partial t} + (u + 1)(u - m)(u - 1), \qquad 0 \geqq m > -1; \\ \text{on the line } t = 0, \; u = -1; \\ \text{on the line } x = 0, \; u = F(t)\text{: given.} \end{cases} \tag{6}$$

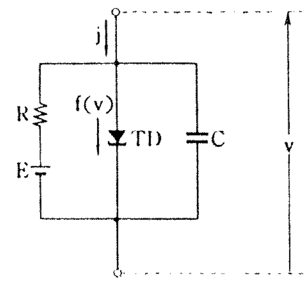

Fig. 1. Basic circuit of the simple bistable line.

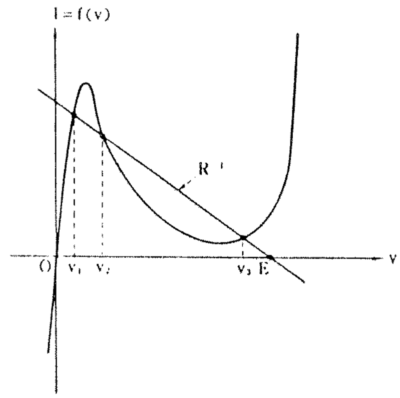

Fig. 2. Bias voltage E and resistance R were set so that the circuit in Fig. 1 performs as a bistable circuit.

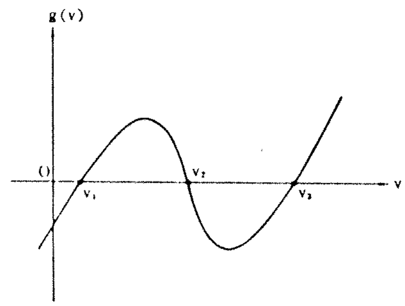

Fig. 3. The function $g(v)$ takes, in general, a form represented by a third-order polynomial (2).

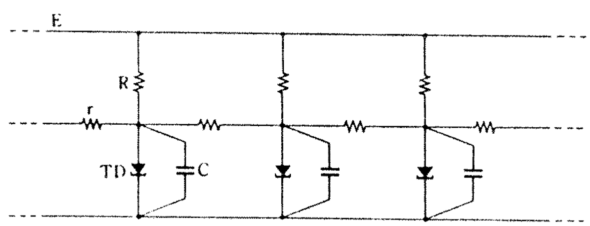

Fig. 4. The simple bistable line is constructed by cascading many of the two-terminal circuits shown in Fig. 1, through interstage coupling resistances.

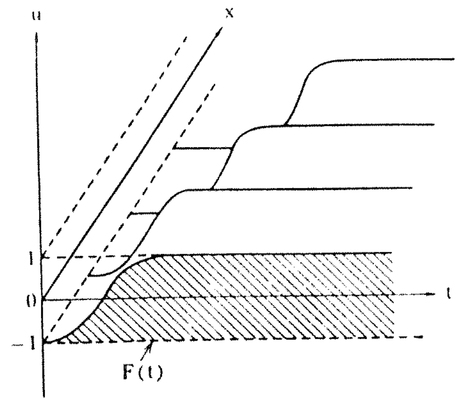

Fig. 5. A schematic display of the boundary-value problem (6).

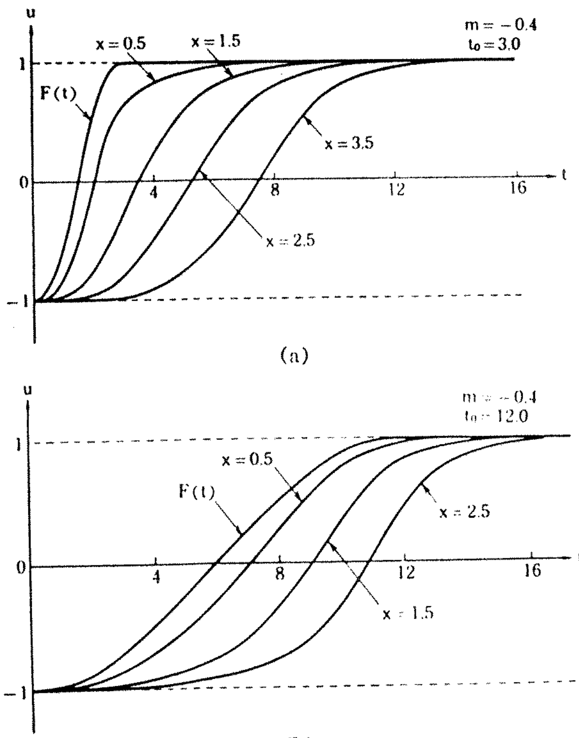

(b)

Fig. 6. Some results of numerical computation of boundary-value problem (6) with boundary condition (7). In these cases, transition waveforms are shaped during their transmission and approach a definite waveform asymptotically.

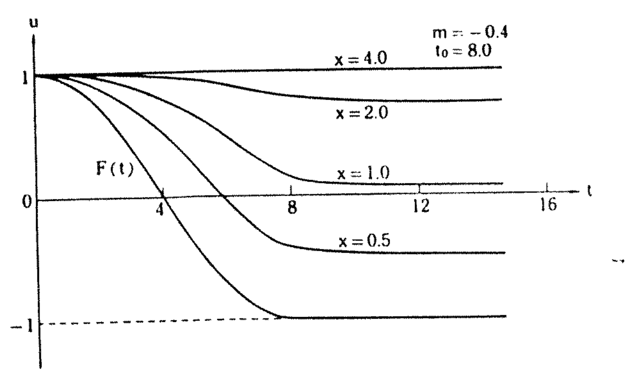

Fig. 7. The transition disappears during transmission in case boundary condition (8) is used. This case is equivalent to one shown in Fig. 6 with $m = 0.4$.

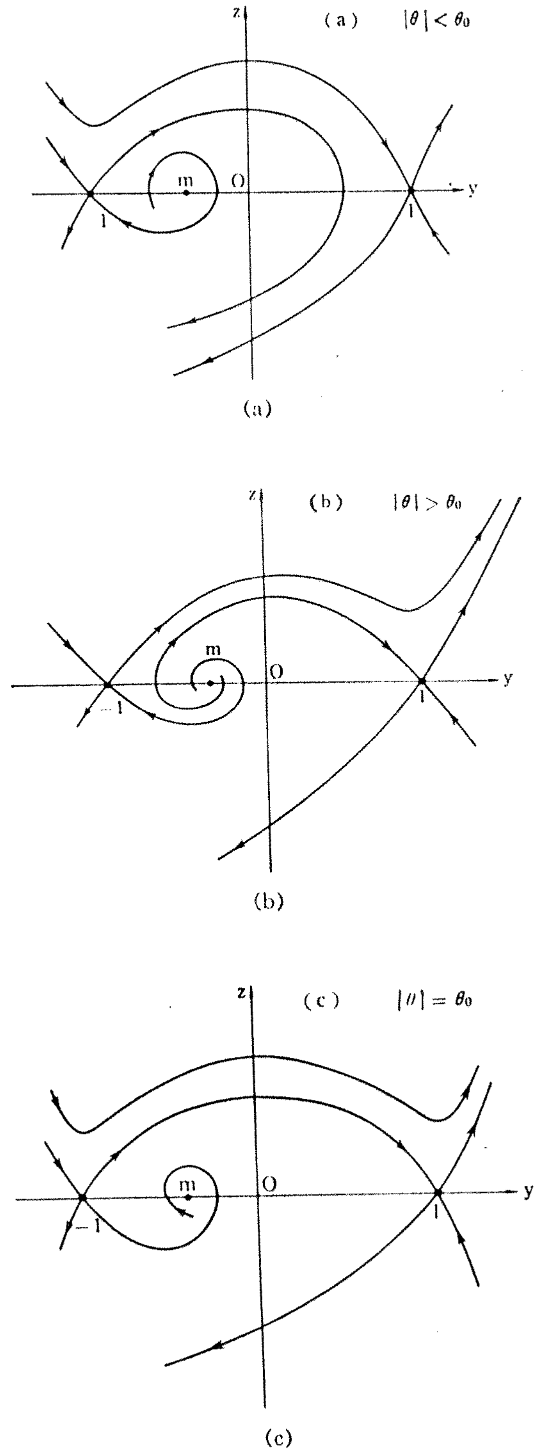

(c)

Fig. 8. Schematic display of the phase portraits of (10) for various values of the parameter θ.

Some results of numerical calculation, using a digital computer, are shown in Fig. 6, where the value $m = -0.4$ is chosen, and

$$\begin{cases} F(t) = -\cos\dfrac{\pi t}{t_0}, & t_0 \geqq t \geqq 0, \\ \quad = 1, & t \geq t_0. \end{cases} \tag{7}$$

From these results, it seems to indicate that the transition waveform is shaped during its transmission and asymptotically approaches a definite waveform inherent to this line.

Next, we shall consider the case of the inverse transition. Keeping the state of the line in the stable state $u = 1$ initially, an appropriate input applied at one end of the line will cause a transition of the state at that end from $u = 1$ to $u = -1$.

Some results of numerical computation are shown in Fig. 7, where $m = -0.4$ as before, and

$$\begin{cases} F(t) = \cos\dfrac{\pi t}{t_0}, & t_0 \geqq t \geqq 0, \\ \quad = -1, & t \geq t_0. \end{cases} \tag{8}$$

From this result, it seems that the transition disappears during transmission, so that it does not approach a definite waveform.

C. Inherent Waveform

If the partial differential equation (5) has a waveform as its solution, which is transmitted along the line without suffering distortion and with a constant velocity (say θ), then the solution must be a function of a single variable $\eta = t - x/\theta$. In such a case, the substitution

$$y(\eta) = u(x, t), \qquad \eta = t - \frac{x}{\theta}$$

reduces the partial differential equation to an ordinary differential equation for y:

$$\frac{1}{\theta^2}\frac{d^2y}{d\eta^2} - \frac{dy}{d\eta} - (y + 1)(y - m)(y - 1) = 0, \tag{9}$$

or

$$\begin{cases} \dfrac{dy}{d\eta} = z, \\ \dfrac{dz}{d\eta} = \theta^2[(y + 1)(y - m)(y - 1) + z], \end{cases} \tag{10}$$

where

$$0 \geqq m > -1.$$

For the time being, θ remains an unknown constant. In fact, its determination constitutes a part of the object of the following procedure.

The system of (10) has three equilibrium points in the phase plane (y–z plane), namely, $(-1, 0)$, $(1, 0)$, and $(m, 0)$. The former two are saddle points (unstable) and the latter is

$$\begin{aligned} &\text{an unstable nodal point if } \theta^2 \geqq 4(1 - m^2), \\ &\text{an unstable focal point if } \theta^2 < 4(1 - m^2). \end{aligned} \tag{11}$$

The trajectory on the phase plane corresponding to the inherent waveform is that which leaves one saddle point and arrives at the other saddle point.

Some phase portraits are schematically shown in Fig. 8. Fig. 8(a) is the case where $|\theta|$ is less than a definite positive value θ_0 (discussed later), Fig. 8(b) is the case where $|\theta| > \theta_0$, and Fig. 8(c) is the case where $|\theta| = \theta_0$. In case $|\theta|$ is exactly equal to θ_0, a trajectory exists which leaves saddle point $(-1, 0)$ and arrives at saddle point $(1, 0)$. On the other hand, for all values of θ, there is no trajectory leaving $(1, 0)$ and arriving at $(-1, 0)$. Moreover, there is no trajectory leaving one of the two saddle points and returning to the same saddle point. (See Appendix.)

These results correspond to the results of the numerical computation of partial differential equation (5). Namely, the existence of an inherent waveform corresponding to the transition from $u = -1$ to $u = 1$ appears to mean that the transition is transmitted along the line, and the nonexistence of the inherent waveform from $u = 1$ to $u = -1$ appears to mean that the transition disappears during transmission.

It is obvious from the final paragraph of Section II-A that, if $1 > m > 0$, only the inherent waveform which corresponds to the transition from $u = 1$ to $u = -1$ exists. Hence, only such a transition will be transmitted along the line.

A. F. Huxley [2] showed that one can obtain the solution of (5), which corresponds to the inherent waveform, by quadrature. We shall try to find the solution following his method.

From (10),

$$\frac{dz}{dy} = \theta^2\left[1 + \frac{(y + 1)(y - m)(y - 1)}{z}\right] \quad (0 > m > -1). \tag{12}$$

Assuming that

$$z = b_0(1 - y^2), \tag{13}$$

where b_0 is an unknown constant, and introducing (13) into (12), we get

$$\begin{cases} \theta = \pm\theta_0, \\ \theta_0 = -\sqrt{2}m > 0, \end{cases} \tag{14}$$

and

$$b_0 = -m > 0. \tag{15}$$

This means that, if $\theta = \pm\,\theta_0$, then (12) has the solution:

$$z = -m(1 - y^2). \tag{16}$$

Since $m < 0$, (16) corresponds to the trajectory which leaves $(-1, 0)$ and arrives at $(1, 0)$.

If θ_0 of (14) is used in (11), the unstable equilibrium point $(m, 0)$ is a focal point if

$$|m| < 0.816, \tag{17}$$

and otherwise a nodal point.

From (10) and (16), one has

$$\frac{dy}{d\eta} = -m(1 - y^2). \tag{18}$$

Setting the initial condition as

$$y = 0 \quad \text{at} \quad \eta = 0,$$

one obtains

$$y(\eta) = -\tanh(m\eta). \tag{19}$$

Thus the inherent waveform is found to be

$$u(x, t) = \tanh\left[-m\left(t + \frac{x}{\sqrt{2m}}\right)\right]. \tag{20}$$

For a fixed x, $u \to 1$ as $t \to +\infty$, and $u = -1$ as $t \to -\infty$.

It should be pointed out that when $m = 0$ (symmetric case), the inherent waveform does not exist.

D. Experiments

To verify the analysis, a lumped constant cascading circuit was constructed as shown in Fig. 9, in which the bias voltage E was used to vary the value of m in (5). Using this line, the following properties regarding signal transmission were observed.

When the bias voltage E is chosen so that $m < 0$, the transition from the stable state in the lower level to that in the higher level travels along the line (Fig. 10); the inverse transition does not (Fig. 11). In Fig. 10 the shaping of the transition waveform is evident.

The transmission velocity increases as the bias voltage increases, that is, as $-m$ increases.

When the bias voltage E is chosen so that $m > 0$, we have the inverse situation.

E. Remarks

It may be concluded from the results in Sections II-C and II-D that, if point v_2 in Fig. 3 is located to the left (right) of the middle point of v_1 and v_3, the transition from $v_1(v_3)$ to $v_3(v_1)$ is transmitted along the line, but the transition from $v_3(v_1)$ to $v_1(v_3)$ is not transmitted. Moreover, if v_2 is exactly at the middle point (symmetric case), there is no transmission of the transition.

Consequently, if we wish to transmit both transitions alternately, some circuit parameters must be changed each time. For example, if we increase the bias voltage E, only the transition from v_1 to v_3 can be transmitted along the line; while if we decrease E, the inverse transition becomes possible. In case of a transmission line using a tunnel diode pair [3], [4] (Fig. 12), we have to set $E_1 < E_2$ and $E_1 > E_2$ alternately in order to transmit each transition.

This inconvenience is avoided by adding a parallel inductance L to the original circuit, as shown in Fig. 13

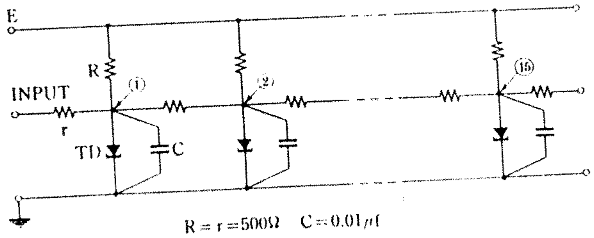

Fig. 9. The circuit used in our experiments.

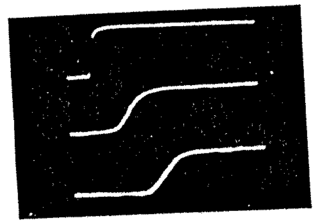

Fig. 10. The transition from the lower stable state to the higher travels along the line and its waveform approaches a definite waveform asymptotically. The waveforms in the first, second, and third lines are those observed at the first, fifth, and ninth stages in the circuit shown in Fig. 9, respectively.

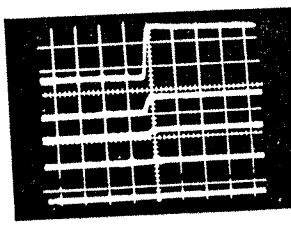

Fig. 11. The transition from the higher to the lower stable state disappears during transmission. The waveforms in the first, second, third, fourth, and fifth lines are those observed at the first, second, third, fourth, and fifth stages in the circuit shown in Fig. 9, respectively.

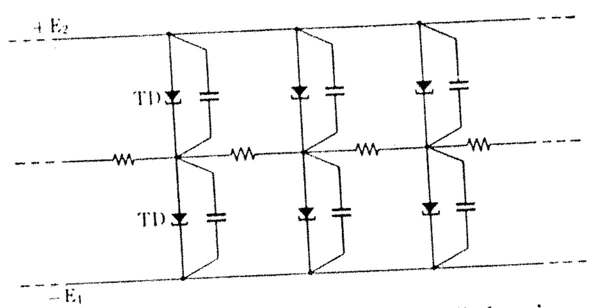

Fig. 12. Bistable line (A) using tunnel diode pairs.

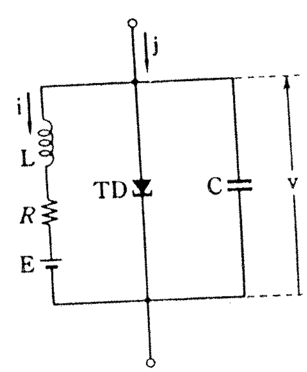

Fig. 13. Basic circuit of the bistable line (B) is obtained by adding an inductance L to the circuit shown in Fig. 1.

[5], [6]. A transmission line with such a structure will be discussed in Section III.

III. Bistable Line (B)

A bistable transmission line will be discussed in this section, in which both transitions (from the lower state to the higher and the inverse) can be transmitted along the line.

A. The circuit and its Equation

We shall consider the circuit in Fig. 14 using a tunnel diode pair, where TD_1 and TD_2 are tunnel diodes with the voltage-current characteristics $I = f_1(v)$ and $I = f_2(v)$, respectively. It is obvious that this circuit is essentially equivalent to that in Fig. 13.

The equation of this circuit is given by

$$\begin{cases} j = C\dfrac{dv}{d\tau} + F(v) + i, \qquad L\dfrac{di}{d\tau} + Ri = v, \\ C = C_1 + C_2, \quad F(v) = f_1(v + E_1) - f_2(E_2 - v). \end{cases} \tag{21}$$

If the bias voltages E_1 and E_2, and resistance R are chosen properly [Fig. 15(a) and (b)], the function

$$g(v) = F(v) + \frac{v}{R} = [f_1(v + E_1) - f_2(E_2 - v)] + \frac{v}{R} \tag{22}$$

takes the form shown in Fig. 16. Let $g(v)$ be represented by a third-order polynomial:

$$g(v) = a(v - v_1)(v - v_2)(v - v_3), \tag{23}$$

where $a > 0$ and $v_1 < v_2 < v_3$.

In case $j = 0$, introducing new variables:

$$u = 2\frac{v - v_1}{v_3 - v_1} - 1, \qquad t = \frac{R}{L}\tau, \tag{24}$$

we have, from (21), (22), (23), and (24),

$$\sigma\frac{d^2u}{dt^2} + (3u^2 - 2mu + \epsilon)\frac{du}{dt} + (u - 1)(u - m)(u + 1) = 0, \tag{25}$$

or

$$\begin{cases} \dfrac{du}{dt} = w, \\ \dfrac{dw}{dt} = -\dfrac{1}{\sigma}\left\{(3u^2 - 2mu + \epsilon)w + (u - 1)(u - m)(u + 1)\right\}, \end{cases} \tag{26}$$

where

$$m = \frac{2v_2 - (v_1 + v_3)}{v_3 - v_1} \qquad (-1 < m < 1),$$

$$\sigma = \frac{RC}{La\left(\dfrac{v_3 - v_1}{2}\right)^2} \qquad (\sigma > 0), \tag{27}$$

$$\epsilon = \frac{RC - L/R}{La\left(\dfrac{v_3 - v_1}{2}\right)^2} - 1 = \sigma\left(1 - \frac{L/R}{RC}\right) - 1.$$

System (26) has three equilibrium points $(-1, 0)$, $(m, 0)$, and $(1, 0)$ in the phase plane (u–w plane). Of these, $(m, 0)$ is a saddle point (unstable) and the other two are, respectively,

stable nodal points if $3 \pm 2m + \epsilon \geqq \sqrt{8\sigma(1 \pm m)}$,

stable focal points if

$$\sqrt{8\sigma(1 \pm m)} > 3 \pm 2m + \epsilon > 0,$$

unstable equilibrium points if $3 \pm 2m + \epsilon < 0$,

where the upper signs are taken for $(-1, 0)$ and the lower signs for $(1, 0)$. Since we are interested in a bistable line, assume

$$3 - 2|m| + \epsilon > 0. \tag{28}$$

Consider a bistable line, with the structure shown in Fig. 17, which is constructed by cascading the many circuits of Fig. 14 through interstage coupling resistances. By considering it is a distributed line, we have

$$j = \frac{1}{r}\frac{\partial v^2}{\partial s^2}, \tag{29}$$

where r is the interstage coupling resistance per unit length of the line and s is the distance along the line. From (21) and (29) it follows that

$$\frac{L}{r}\frac{\partial^3 v}{\partial\tau\partial s^2} + \frac{R}{r}\frac{\partial^2 v}{\partial s^2} = LC\frac{\partial^2 v}{\partial\tau^2} + (LF'(v) + RC)\frac{\partial v}{\partial\tau} + (v + RF(v)). \tag{30}$$

Using the expression of $g(v)$ in (23) and the new variables

$$x = \sqrt{ra}\left(\frac{v_3 - v_1}{2}\right)s, \qquad u = 2\frac{v - v_1}{v_3 - v_1} - 1, \qquad t = \frac{R}{L}\tau, \tag{31}$$

we have the following fundamental equation:

$$\frac{\partial^3 u}{\partial t\,\partial x^2} + \frac{\partial^2 u}{\partial x^2} = \sigma\frac{\partial^2 u}{\partial t^2} + (3u^2 - 2mu + \epsilon)\frac{\partial u}{\partial t} + (u - 1)(u - m)(u + 1), \tag{32}$$

where $\sigma > 0$, $|m| < 1$, and $3 - 2|m| + \epsilon > 0$.

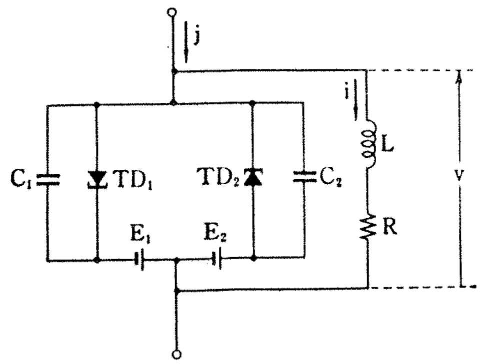

Fig. 14. Basic circuit of the bistable line (B), where a tunnel diode pair is used.

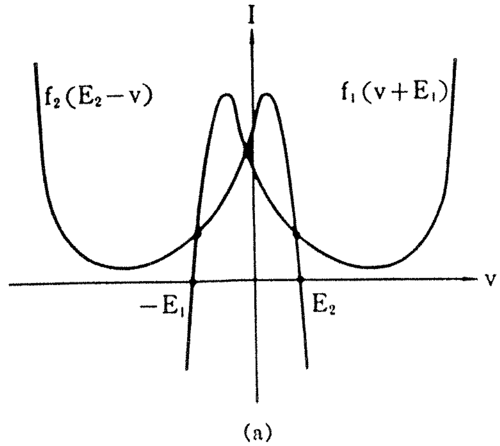

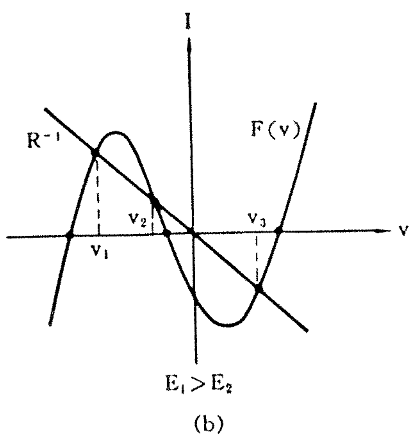

Fig. 15. The bias voltages E_1 and E_2 and the resistance R must be chosen so that $g(v)$ in (22) has the form shown in Fig. 16.

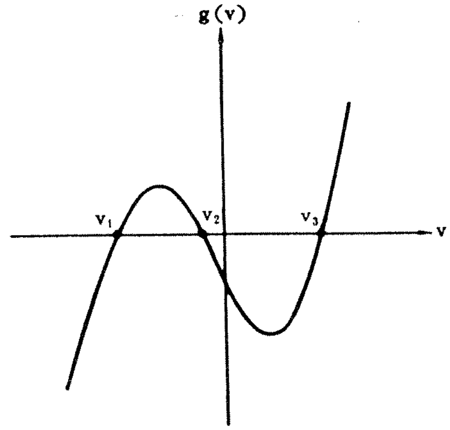

Fig. 16. The function $g(v)$ takes, in general, a form which is represented by a third-order polynomial (23).

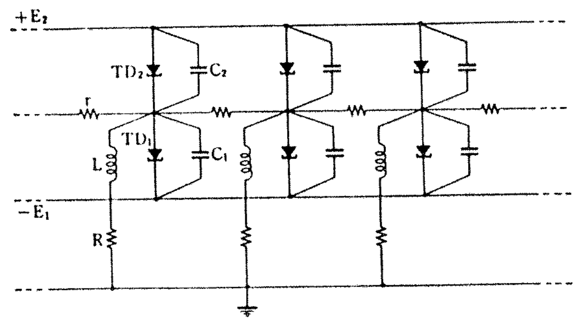

Fig. 17. The bistable line is constructed by cascading many of the two-terminal circuits shown in Fig. 14, through interstage coupling resistances.

B. Propagation of Transition and Boundary-Value Problem

Partial differential equation (32) has three constant solutions: $u = -1$, 1, and m. The first two correspond to stable equilibrium states and the latter to the unstable equilibrium state.

We shall consider the propagation of the transition from one state to the other as in Section II-B. In this case, we expect that both transitions (from $u = -1$ to $u = 1$ and from $u = 1$ to $u = -1$) are possible. This expectation is proved by solving the following boundary-value problem:

$$\begin{cases} u = u(x,t), \quad x \geqq 0, \quad t \geqq 0; \\ \dfrac{\partial^3 u}{\partial t\,\partial x^2} + \dfrac{\partial^2 u}{\partial x^2} = \sigma \dfrac{\partial^2 u}{\partial t^2} + (3u^2 - 2mu + \epsilon)\dfrac{\partial u}{\partial t} \\ \qquad\qquad + (u-1)(u-m)(u+1); \\ \sigma > 0, \quad |m| < 1, \quad 3 - 2|m| + \epsilon > 0; \\ \text{on the line } t = 0, \quad \dfrac{\partial u}{\partial t} = 0, \quad u = -1 (\text{or } 1); \\ \text{on the line } x = 0, \quad u = F(t) : \text{given}. \end{cases} \tag{33}$$

Some results of numerical calculation, using a digital computer, are shown in Figs. 18 and 19. Here, $u = -1$ at $t = 0$, and

$$\begin{cases} F(t) = -\cos\left(\dfrac{\pi t}{t_0}\right), & t_0 \geqq t \geqq 0, \\ \quad\;\; = 1, & t \geqq t_0. \end{cases} \tag{34}$$

When $m = 0$, -0.1, and -0.3, transmissions of the transition were observed.

In case of the transition from $u = 1$ to $u = -1$, similar results were obtained when $m = -0.1$, as shown in Fig. 20(a), while the transition from $u = 1$ to $u = -1$ disappeared when $m = -0.3$, as shown in Fig. 20(b). From these computations, we may conclude that:

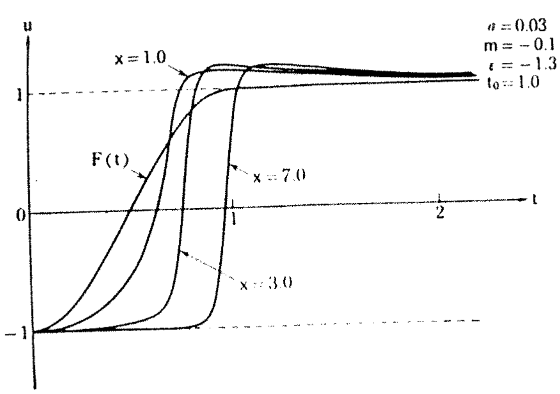

Fig. 18. Some results of numerical computation in a symmetric case of boundary-value problem (33) with boundary condition (34), where the transition waveform is shaped during transmission and approaches a definite waveform asymptotically.

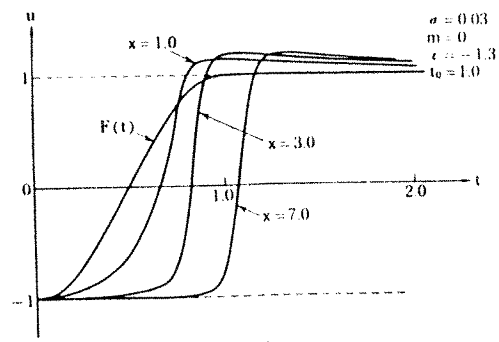

(a)

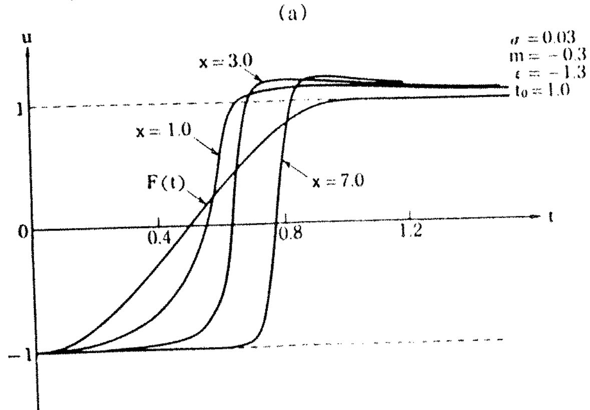

(b)

Fig. 19. Some results of numerical computation in an asymmetric case.

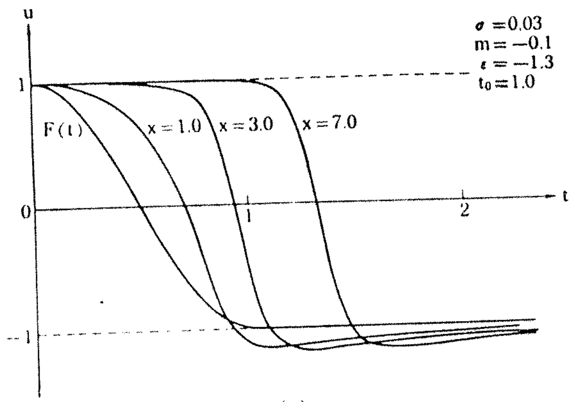

(a)

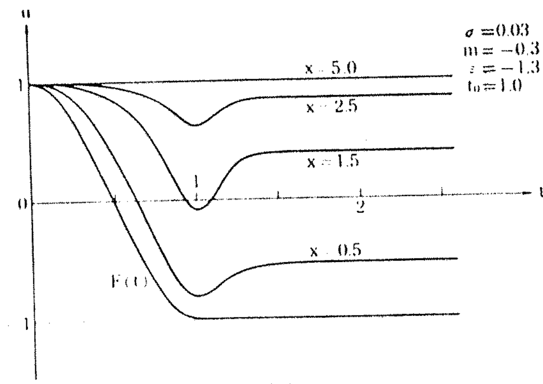

(b)

Fig. 20. (a) When $m = -0.1$, the transition from $u = 1$ to $u = -1$ travels along the line similarly as that from $u = -1$ to $u = 1$ [Fig. 19(a)]. (b) When $m = -0.3$, the transition from $u = 1$ to $u = -1$ disappears. Note that the transition from $u = -1$ to $u = 1$ can travel [Fig. 19(b)].

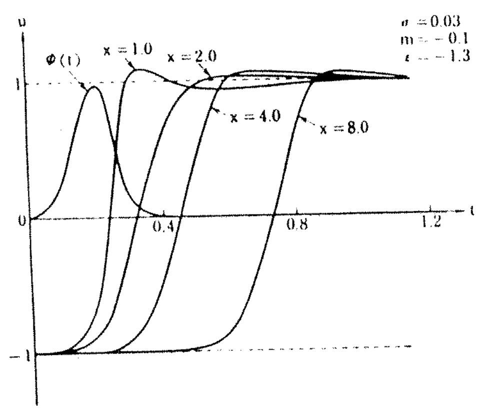

Fig. 21. Some results of numerical computation of boundary-value problem (33) with boundary condition (36). In this case,

$$\begin{cases} \Phi(t) = \frac{1}{2}(1 - \cos 5\pi t), & 0.4 \geqq t \geqq 0, \\ \quad = 0, & t > 0.4. \end{cases}$$

1) If the structure of the transmission line is almost symmetrical, that is, $|m| < m_0$ (where m_0 is a positive constant), this line can transmit both transitions (from $u = -1$ to $u = 1$ and from $u = 1$ to $u \doteq -1$).
2) As the degree of asymmetry of the transmission line increases, that is, as $|m|$ increases, only one transition travels along that line. More precisely, it can be said that, if $m < -m_0$, the transition from -1 to 1 travels along the line, while the transition from 1 to -1 does not. If $m > m_0$ the inverse situation holds.
3) When the transition is transmitted along the line, the propagating waveform takes shape and approaches a peculiar transition waveform (a waveform inherent to the line) during transmission. The peculiar transition waveform travels the line without suffering distortion and at a constant velocity.

Next, we shall consider the case where the line is triggered by a current source at one end. Then, at $s = 0$,

$$\frac{\partial v}{\partial s} = r\varphi(\tau), \tag{35}$$

where $\varphi(\tau)$ is the triggering current. Thus, the last condition of boundary-value problem (33) is replaced by

$$\text{on the line } x = 0, \qquad \frac{\partial u}{\partial x} = \Phi(t) : \text{given}, \tag{36}$$

where

$$\Phi(t) = \sqrt{\frac{r}{a}}\left(\frac{2}{v_3 - v_1}\right)^2 \varphi\left(\frac{L}{R}\,t\right). \tag{37}$$

Some results of numerical computation on boundary-value problem (33) using (36), are shown in Fig. 21.

C. Inherent Waveform

Applying the same procedure as in Section II-C to (32), one obtains the following ordinary differential equation:

$$\beta\frac{d^3\xi}{d\eta^3} + (\beta - \sigma)\frac{d^2\xi}{d\eta^2} - (3\xi^2 - 2m\xi + \epsilon)\frac{d\xi}{d\eta} - (\xi - 1)(\xi - m)(\xi + 1) = 0, \tag{38}$$

where

$$u(x, t) = \xi(\eta), \qquad \eta = t - \frac{x}{\theta}, \quad \text{and} \quad \beta = \theta^{-2}.$$

Equation (38) has three constant solutions, $\xi = -1$, m, and 1, corresponding to three constant solutions $u = -1$, m, and 1 of partial differential equation (32), respectively.

Now, if (38) has a solution such as $\xi(\eta) \to -1$ as $\eta \to -\infty$ and $\xi(\eta) \to 1$ as $\eta \to +\infty$ for some value of θ, as shown in Fig. 22, then this solution corresponds to the inherent waveform we are seeking, and the transmission velocity is determined from the value of θ.

At first, we shall consider the behavior of $\xi(\eta)$ in some neighborhoods of equilibrium points $\xi = \pm 1$. Near solution $\xi = -1$, (38) is approximated by a linear differential equation

$$\beta\frac{d^3y}{d\eta^3} + (\beta - \sigma)\frac{d^2y}{d\eta^2} - (3 + 2m + \epsilon)\frac{dy}{d\eta} - 2(1 + m)y = 0, \tag{39}$$

where $y = \xi + 1$. The characteristic equation of (39):

$$H(\lambda) \equiv \beta\lambda^3 + (\beta - \sigma)\lambda^2 - (3 + 2m + \epsilon)\lambda - 2(1 + m) = 0 \tag{40}$$

has only one real positive root, since $H(+\infty) = +\infty$,

$$H(0) = -2(1 + m) < 0 \quad \text{and} \quad H'(0) = -(3 + 2m + \epsilon) < 0.$$

Denoting this root by $\lambda_0(\lambda_0 > 0)$, $H(\lambda)$ is factorized as

$$H(\lambda) = (\lambda - \lambda_0)(\beta\lambda^2 + \gamma\lambda + 2(1 + m)\lambda_0^{-1}),$$

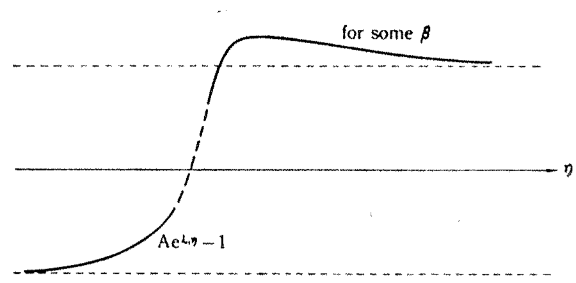

Fig. 22. If (38) has a solution such as $\xi(\eta) \to -1$ as $\eta \to -\infty$ and $\xi(\eta) \to 1$ as $\eta \to +\infty$, for some value of θ, this solution corresponds to the inherent waveform we are seeking, and the transmission velocity is determined from the θ.

where

$$\gamma = (\lambda_0 + 1)\beta - \sigma = 2(1 + m)\lambda_0^{-2} + (3 + 2m + \epsilon)\lambda_0^{-1}.$$

Since $\gamma > 0$, it is apparent that both the other two roots are either real negative or complex conjugate with negative real parts.

Near solution $\xi = 1$, (38) is approximated by

$$\beta\frac{d^3y}{d\eta^3} + (\beta - \sigma)\frac{d^2y}{d\eta^2} - (3 - 2m + \epsilon)\frac{dy}{d\eta} - 2(1 - m)y = 0, \tag{41}$$

where $y = \xi - 1$. By the same procedure as previously mentioned, it is found that the characteristic equation of (41) has one real positive root and either two real negative roots or complex conjugate roots with negative real parts.

If $\xi(\eta) \to -1$ as $\eta \to -\infty$, as shown in Fig. 22, then

$$\xi(\eta) \sim -1 + Ae^{\lambda_0\eta},$$

where η takes a large negative value and A is an arbitary constant. Moreover,

$$\xi'(\eta) \sim A\lambda_0 e^{\lambda_0\eta}, \qquad \xi''(\eta) \sim A\lambda_0^2 e^{\lambda_0\eta}.$$

Thus, varying the value of β, we seek the solution $\xi(\eta)$ such as $\xi(\eta) \to 1$ as $\eta \to \infty$ by numerical calculations for the third-order differential equation (38), beginning with the following initial conditions:

$$\xi(0) = -1 + \Delta, \quad \xi'(0) = \lambda_0\Delta, \quad \xi''(0) = \lambda_0^2\Delta, \tag{42}$$

where $1 \gg \Delta > 0$. Note that λ_0 depends on β.

Some results of numerical calculation are shown in Fig. 23 for $\sigma = 0.03$, $\epsilon = -1.3$, and for $m = 0$ and $m = -0.1$. Figure 24 shows the relation between the transmission velocity θ and the value of m. In Fig. 25 the relations between θ and σ are shown.

From these results, we have the following conclusions corresponding to those in Section III-B.

1) If $|m|$ is small, two solutions exist side by side, one of which satisfies $\xi(-\infty) = -1$ and $\xi(+\infty) = 1$;

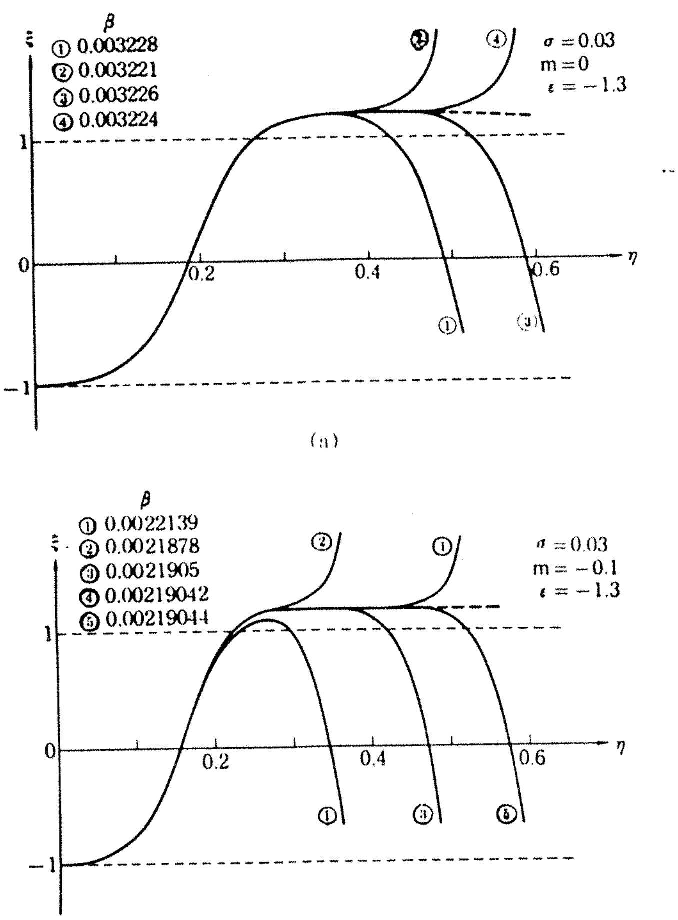

(a)

(b)

Fig. 23. Inherent waveform obtained by numerical computation for the third-order differential equation (38).

the other $\xi(-\infty) = 1$ and $\xi(+\infty) = -1$.

2) If $|m|$ is large, there is only one solution. More precisely, when $m < -m_0'$ (m_0' is a positive constant), only the solution which satisfies $\xi(-\infty) = -1$ and $\xi(+\infty) = 1$ exists, while the solution which satisfies $\xi(-\infty) = 1$, and $\xi(+\infty) = -1$ does not. When $m > m_0'$, the inverse situation holds.

3) The numerically obtained waveforms of (32) [see, for example, Fig. 19] approach asymptotically the inherent waveform which is a solution of (38).

D. Experiments

We fabricated a lumped constant cascaded circuit (ten stages of the bistable circuit) as shown in Fig. 26 to simulate a distributed bistable line. Figure 27(b) shows the form of the function

$$F(v) = f(v + E_1) - f(E_2 - v),$$

which is obtained from the $v - I$ characteristic of the tunnel diodes shown in Fig. 27(a). The curve ① in Fig. 27(b) is symmetric ($E_1 = E_2$), and the curve ② is asymmetric ($E_1 < E_2$).

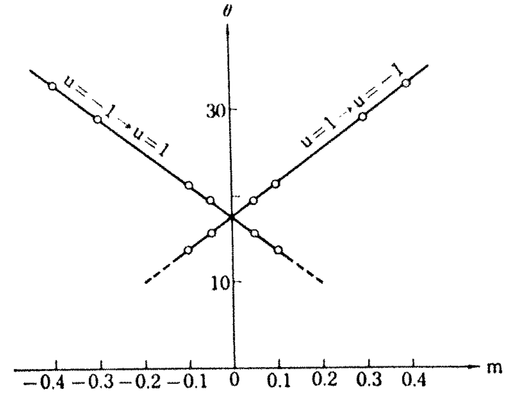

Fig. 24. The relation between the transmission velocity θ and the value of m.

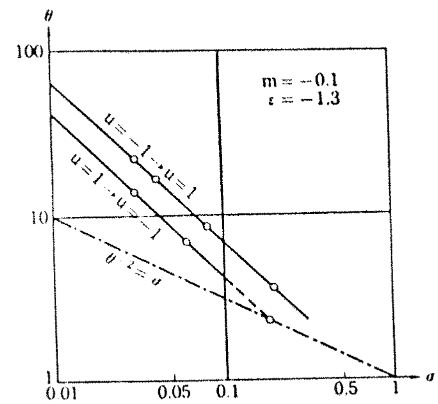

Fig. 25. The relations between θ and σ.

Figure 28 shows the waveform shaping process of this circuit.

The transmission time of the transition along the line is shown in Table I.

E. Results of Other Experiments

We shall describe the results of other experiments using the circuit in Fig. 26.

1) When the two bias voltages E_1 and E_2 are not equal, the characteristic curve of the tunnel diode pair is asymmetric, as shown in Fig. 27(b). This makes the transmission velocities for the two transitions (from the lower state to the higher and from the higher state to the lower) unequal. Hence, the widths of rectangular pulses change during transmission, as shown in Fig. 29. This phenomenon might be utilized for prolonging and compressing pulse width, for example, in PWM.

2) Keeping the line initially at the stable equilibrium state $u = -1$, we apply a step input at one end of the line, fixing the other at $u = -1$. In this case, transition travels to and fro along the line so that free oscillation takes place, as shown by experiment, in Fig. 30, or by computation, in Fig. 31.

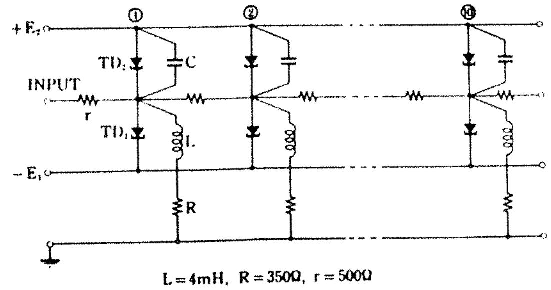

Fig. 26. The circuit used in our experiments.

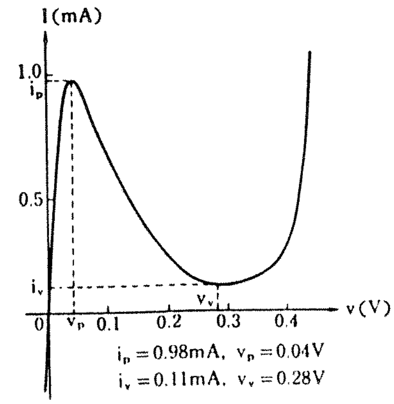

(a)

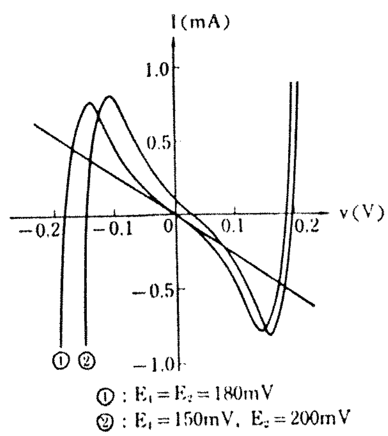

(b)

Fig. 27. (a) $v - I$ characteristic curve $I = f(v)$ of the tunnel diode used. (b) $F(v) = f(v + E_1) - f(E_2 - v)$ is calculated from (a). The curve ① is the case $E_1 = E_2$, and the curve ② is the case $E_1 > E_2$.

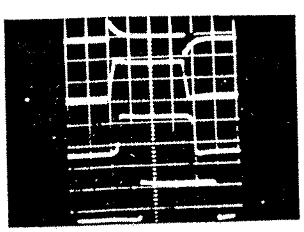

Fig. 28. The process of waveform shaping. The waveforms in the first, second, third, and fourth lines are those observed at the input terminal, the first, third, and tenth stages of the circuit in Fig. 26 with $E_1 = E_2 = 220$ mV, $C = 30$ pf, respectively. Pulse height in the first line is 70 mV, and those in the second, third, and fourth are 45 mV, 40 mV, and 40 mV, respectively. Pulse width in the bottom line is 180 μsec.

TABLE I

THE TRANSMISSION TIME OF THE TRANSITION ALONG THE LINE

Delay (μsec)		$C(\mu f)$ 0.004	0.01
$E_1 = E_2 = E_0$	0.18	48	86
(V)	0.2	21	70

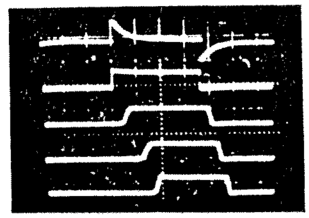

(a)

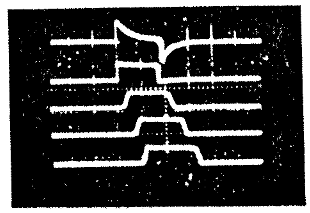

(b)

Fig. 29. The widths of the rectangular pulses change during transmission if E_1 and E_2 in Fig. 26 are not equal. (a) In case of $E_1 = 190$ mV, $E_2 = 200$ mV, a wide pulse with 180 μsec width is narrowed in th course of transmission. Pulse width in the bottom line is 150 μsec. (b) In case of $E_1 = 220$ mV, $E_2 = 170$ mV, a narrow pulse with 180 μsec width is widened in the course of transmission. Pulse width in the bottom line is 220 μsec. In each figure, the first waveform is that of input triggering; the second, third, fourth, and the fifth waveforms are those observed at the first, fourth, seventh, and the ninth stages, respectively. In both cases, $C = 0.01$ μf.

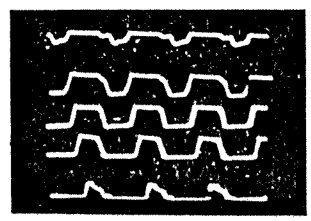

Fig. 30. Free oscillation observed in the circuit in Fig. 26 with $E_1 = E_2 = 220$ mV, $C = 0.01$ μf. The waveforms in the first, second, third, fourth, and fifth lines are those observed at the second, fourth, sixth, eighth, and tenth stages, respectively. The period of this oscillation is 120 μsec.

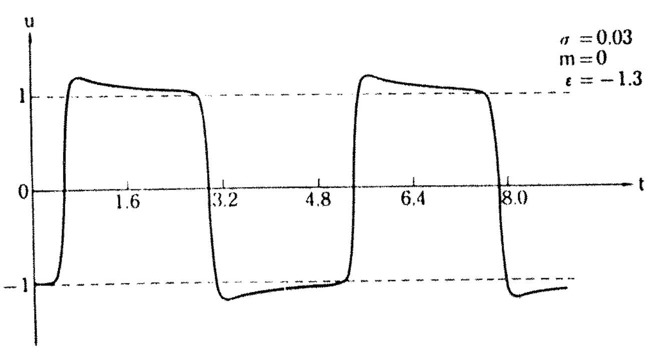

Fig. 31. Free oscillation obtained by numerical computation.

Appendix

The following four statements mentioned in Section II-C will be proved:

a) For all values of θ and m, such as $\theta \neq 0, 0 > m > -1$, (10) has no trajectory leaving the saddle point (1, 0) and arriving at the other saddle point (−1, 0).

b) For $|\theta| > \theta_0$, where $\theta_0 = -\sqrt{2}\, m$, the trajectory of (10) which leaves the saddle point (−1, 0) to the right crosses the line $y = 1$ at a point above the y axis, as shown in Fig. 8(b).

c) For $|\theta| < \theta_0$, where $\theta_0 = -\sqrt{2}\, m$, the trajectory of (10) which leaves the saddle point (−1, 0) to the right crosses the y axis at a point left of $y = 1$, as shown in Fig. 8(a).

If these three statements are proved, we have the conclusion that, for $\theta = \theta_0(\theta_0 = -\sqrt{2}\, m)$, (10) has a trajectory leaving the saddle point (−1, 0) and arriving at the other saddle point (1, 0) as shown in Fig. 8(c), and that this is the only trajectory connecting the two saddle points. This trajectory corresponds to Huxley's solution.

d) There is no trajectory which leaves one of the two saddle points and returns to the same saddle point.

Proof of a)

Consider a parabola:

$$z = \alpha(y^2 - 1) \tag{43}$$

in the interval $1 \geqq y \geqq -1$, where α is a positive constant.

We intend to choose the constant α in (43) so that along all points of the parabola the field vector of (10) points outward from the crescent-shaped area in Fig. 32.

In this case, the trajectory leaving the saddle point (1, 0) through the unstable downward branch never arrives at the other saddle point (−1, 0). In fact, since the vector of (10) always points to the left in the lower half plane and the unstable trajectory leaving the saddle point (−1, 0) to the left goes down to infinity, there is no possibility of the trajectory which leaves (1, 0) arriving at the saddle point (−1, 0) along either of its stable trajectories.

Now, on parabola (43), dz/dy in (12) is given by

$$\frac{dz}{dy} = \theta^2\left(1 + \frac{y - m}{\alpha}\right). \tag{44}$$

On the other hand, the tangent vector of the parabola is given by

$$\frac{dz}{dy} = 2\alpha y. \tag{45}$$

Consequently, if

$$\theta^2\left(1 + \frac{y - m}{\alpha}\right) > 2\alpha y \tag{46}$$

throughout the interval $1 \geqq y \geqq -1$, then the field vector of (10) points outward from the cresent-shaped area along all points of the parabola.

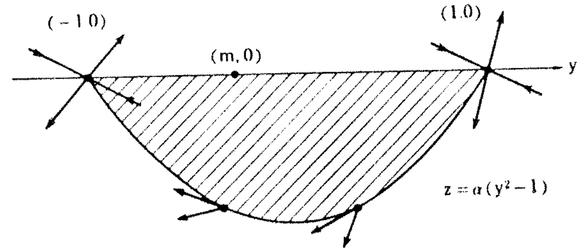

Fig. 32. Along all points of the parabola, the field vector of (10) points outward from the crescent-shaped area, if (46) holds.

Since (46) is a linear inequality for y in the interval $1 \geqq y \geqq -1$, (46) holds for all y in that interval if (46) holds at $y = 1$ and $y = -1$. These conditions lead to

$$\begin{cases} \theta^2\left(1 + \dfrac{1 - m}{\alpha}\right) > 2\alpha, \\ \theta^2\left(1 + \dfrac{-1 - m}{\alpha}\right) > -2\alpha, \end{cases} \tag{47}$$

or

$$\begin{cases} 2\alpha^2 - \theta^2\alpha - \theta^2(1 - m) < 0, \\ 2\alpha^2 + \theta^2\alpha - \theta^2(1 + m) > 0. \end{cases} \tag{48}$$

These inequalities hold simultaneously if

$$\theta^2 + \sqrt{\theta^4 + 8\theta^2(1 - m)} > 4\alpha > -\theta^2 + \sqrt{\theta^4 + 8\theta^2(1 + m)}. \tag{49}$$

Since the left-hand side of (49) is greater than the right-hand side for all values of θ and m such as $\theta \neq 0$, $0 > m > -1$, one can always choose an α which satisfies (49), and statement a) is proved.

Proof of b)

Consider again the parabola (43) with α negative. The process of the proof is the same as that for a). Proceeding as before, we have

$$\begin{cases} 2\alpha^2 - \theta^2\alpha - \theta^2(1 - m) > 0, \\ 2\alpha^2 + \theta^2\alpha - \theta^2(1 + m) < 0, \end{cases} \tag{50}$$

instead of (48). These inequalities hold simultaneously if

$$\theta^2 - \sqrt{\theta^4 + 8\theta^2(1 - m)} > 4\alpha > -\theta^2 - \sqrt{\theta^4 + 8\theta^2(1 + m)}, \tag{51}$$

since α is negative.

In order to be able to choose an α which satisfies (51), it is necessary and sufficient that the difference d:

$$d = [\text{left-hand side of (51)}] - [\text{right-hand side of (51)}] = 2\theta^2 + \sqrt{\theta^4 + 8\theta^2(1 + m)} - \sqrt{\theta^4 + 8\theta^2(1 - m)}$$

be positive. This condition leads to

$$\sqrt{(\theta^2 + 8)^2 - 64m^2} > 8 - \theta^2. \tag{52}$$

if $|\theta| \geqq 2\sqrt{2}$, (52) always holds. On the other hand, if $|\theta| < 2\sqrt{2}$, we know that (52) holds so long as

$$|\theta| > -\sqrt{2}m. \tag{53}$$

Therefore, we come to the conclusion that, if (53) holds, we can choose an α which satisfies (51). This proves statement b).

Proof of c)

In this case, one obtains

$$\theta^2\left(1 + \frac{y - m}{\alpha}\right) < 2\alpha y, \tag{54}$$

instead of (46). (See Fig. 33.)

Proceeding as before, we obtain (48), and hence

$$-\theta^2 - \sqrt{\theta^4 + 8\theta^2(1 + m)} > 4\alpha$$
$$> \theta^2 - \sqrt{\theta^4 + 8\theta^2(1 - m)}, \tag{55}$$

since α is negative. The condition

$$d = -2\theta^2 + \sqrt{\theta^4 + 8\theta^2(1 - m)}$$
$$- \sqrt{\theta^4 + 8\theta^2(1 + m)} > 0$$

leads to

$$8 - \theta^2 > \sqrt{(\theta^2 + 8)^2 - 64m^2}, \tag{56}$$

instead of (52). Since (56) is satisfied if

$$|\theta| < -\sqrt{2}m, \tag{57}$$

statement c) is proved.

Proof of d)

Assuming that there exists a trajectory which leaves one of the two saddle points and returns to the same saddle point for $\theta = \theta_1$, let the corresponding solution of (9) be $y_1(\eta)$. Then

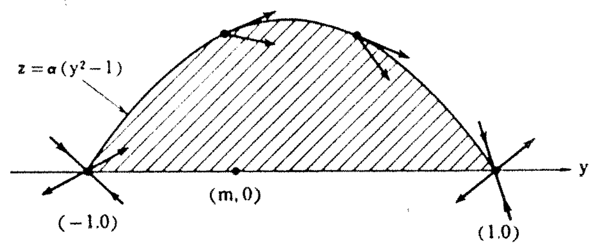

Fig. 33. Along all points of the parabola, the field vector of (10) points inward from the edge of the crescent-shaped area, if (54) holds.

$$\frac{1}{\theta^2}\frac{d^2y_1}{d\eta^2} - \frac{dy_1}{d\eta} - (y_1 + 1)(y_1 - m)(y_1 - 1) = 0. \tag{58}$$

Multiplying both sides of (58) by $dy_1/d\eta$ and integrating from $\eta = -\infty$ to $\eta = \infty$, we obtain

$$\int_{-\infty}^{\infty} \left(\frac{dy_1}{d\eta}\right)^2 d\eta = 0, \tag{59}$$

since $dy_1/d\eta = 0$ at $\eta = \pm\infty$. Equation (59) leads to $dy_1/d\eta = 0$ for all η, which contradicts our assumption.

Acknowledgment

The authors wish to express their thanks to Dr. R. Fitz Hugh, National Institutes of Health, U. S. A., for his kindness in informing us of Huxley's solution and for his valuable discussions.

References

[1] J. Nagumo, S. Arimoto, and S. Yoshizawa, "An active pulse transmission line simulating nerve axon," *Proc. IRE*, vol. 50, pp. 2061–70, October, 1962.

[2] A. F. Huxley, unpublished.

[3] R. S. Mackay, "Negative resistance," *Am. J. Phys.*, vol. 26, pp. 60–69, February, 1958.

[4] E. Goto et al., "Esaki diode high-speed logical circuits," *IRE Trans. on Electronic Computers*, vol. EC-9, pp. 25–29, March, 1960.

[5] S. Yoshizawa and J. Nagumo, "A bistable distributed line," Rept. of Professional Group on Nonlinear Circuit Theory, Inst. Elect. Commun. Engrs., Japan, July 1963, (in Japanese).

[6] S. Yoshizawa and J. Nagumo, "A bistable distributed line," *Proc. IEEE (Correspondence)*, vol. 52, pp. 308, March, 1964.